Quantum Optics Project II

Carey Phelps, Jun Yin and Tim Sweeney
Department of Physics and Oregon Center for Optics
1274 University of Oregon
Eugene, Oregon 97403-1274

15 May 2007

1 Simulation of quantum-state diffusion

The simulation of quantum-state diffusion has been attempted using the Stochastic Schrödinger Equation (SSE) derived from the Stochastic Master Equation (SME) for a two level atom, where the output is monitored by homodyne detection of the X1 quadrature ($\langle x \rangle$).

1.1 Theory

The SME given by

$$d\rho = -\frac{i}{\hbar}[H,\rho]dt + \Gamma\mathcal{D}[\sigma e^{i\phi}]\rho dt + \sqrt{\Gamma}\mathcal{H}[\sigma e^{i\phi}]\rho dW, \tag{1}$$

where the Lindblad superoperator is

$$\mathcal{D}[c]\rho = c\rho c^\dagger - \frac{1}{2}(c^\dagger c\rho + \rho c^\dagger c) \tag{2}$$

and the measurement superoperator is

$$\mathcal{H}[c]\rho = c\rho + \rho c^\dagger - Tr[c\rho + \rho c^\dagger]\rho \tag{3}$$

$$= c\rho + \rho c^\dagger - \langle c\rho + \rho c^\dagger\rangle\rho \tag{4}$$

is equivalent to the SSE

$$d|\psi\rangle = -\frac{i}{\hbar}H|\psi\rangle dt - \frac{\Gamma}{2}[\sigma^\dagger\sigma - \langle\sigma+\sigma^\dagger\rangle\sigma + \frac{1}{4}\langle\sigma+\sigma^\dagger\rangle^2]|\psi\rangle dt + \sqrt{\Gamma}[\sigma - \frac{1}{2}\langle\sigma+\sigma^\dagger\rangle]|\psi\rangle dW \tag{5}$$

if you expand $d\rho$ to second order using Ito's rule.

Lets show it explicitly, first by expanding ρ,

$$d\rho = (d|\psi\rangle)\langle\psi| + |\psi\rangle(d\langle\psi|) + (d|\psi\rangle)(d\langle\psi|). \tag{6}$$

a)

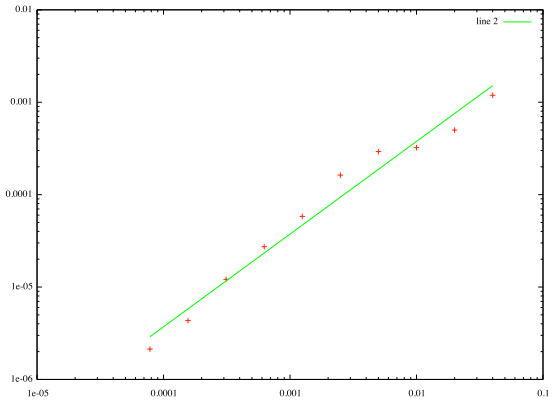

b)

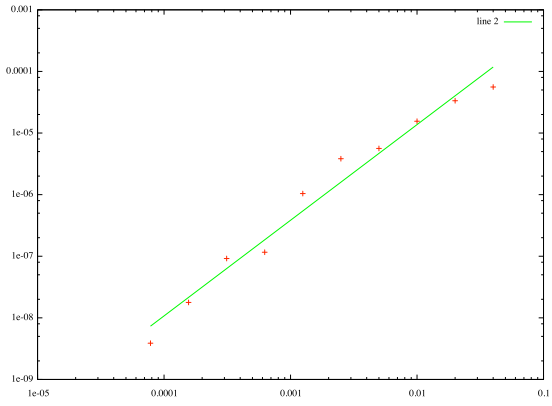

Figure 1: Plotted in a) and b) is error, defined as the mean absolute difference from numerical to analytic solutions verses step size . Graph a), goes as Δt for numerical methods using first-order explicit deterministic integrator and first-order stochastic Runga-Kutta integrator, and b) the error goes as $\Delta t^{1.5}$ for numerical methods using implicit evolution of the deterministic part of the equation, specifically a order 1.5 Runga-Kutta method in Kloeden/Platenand .

We are now going to brake up (6) into its three components and plug in the SSE where we see $d(|\psi\rangle)$ and $d(\langle\psi|)$. Note that $dt^2 = dtdW = 0$ and $dW^2 = dt$.

$$\begin{aligned}
(d|\psi\rangle)\langle\psi| =& -\tfrac{i}{\hbar}H|\psi\rangle\langle\psi|dt - \tfrac{\Gamma}{2}[\sigma^\dagger\sigma - \langle\sigma+\sigma^\dagger\rangle\sigma + \tfrac{1}{4}\langle\sigma+\sigma^\dagger\rangle^2]|\psi\rangle\langle\psi|dt + \sqrt{\Gamma}[\sigma - \tfrac{1}{2}\langle\sigma+\sigma^\dagger\rangle]|\psi\rangle\langle\psi|dW \\
=& -\tfrac{i}{\hbar}H\rho dt - \tfrac{\Gamma}{2}[\sigma^\dagger\sigma - \langle\sigma+\sigma^\dagger\rangle\sigma + \tfrac{1}{4}\langle\sigma+\sigma^\dagger\rangle^2]\rho dt + \sqrt{\Gamma}[\sigma - \tfrac{1}{2}\langle\sigma+\sigma^\dagger\rangle]\rho dW \\
|\psi\rangle(d\langle\psi|) =& \tfrac{i}{\hbar}\rho H dt - \tfrac{\Gamma}{2}\rho[\sigma\sigma^\dagger - \langle\sigma+\sigma^\dagger\rangle\sigma^\dagger + \tfrac{1}{4}\langle\sigma+\sigma^\dagger\rangle^2]dt + \sqrt{\Gamma}\rho[\sigma^\dagger - \tfrac{1}{2}\langle\sigma+\sigma^\dagger\rangle]dW \\
(d|\psi\rangle)(d\langle\psi|) =& \Gamma(\sigma - \tfrac{1}{2}\langle\sigma+\sigma^\dagger\rangle)\rho(\sigma^\dagger - \tfrac{1}{2}\langle\sigma+\sigma^\dagger\rangle)dt \\
=& \Gamma\left[\sigma\rho\sigma^\dagger - \tfrac{1}{2}\langle\sigma+\sigma^\dagger\rangle\rho\sigma^\dagger - \tfrac{1}{2}\langle\sigma+\sigma^\dagger\rangle\sigma\rho + \tfrac{1}{4}\langle\sigma+\sigma^\dagger\rangle^2\rho\right]
\end{aligned} \tag{7}$$

Plugging the equations from (7) into (6) we arrive at the SME.

1.2 Integrator Test

As a test of the program, we studied the error for a given analytic solution to the numerical solution and found great correspondence. In Figure **??** it can be seen that the the error went like Δt for numerical methods using first-order explicit deterministic integrator and first-order stochastic Runga-Kutta integrator, and $\Delta t^{1.5}$ for numerical methods using implicit evolution of the deterministic part of the equation, specifically a order 1.5 Runga-Kutta method in Kloeden/Platenand (I don't really know what that means but I hear it kicks ass), and an order 2 deterministic step for the stochastic part of the equation.

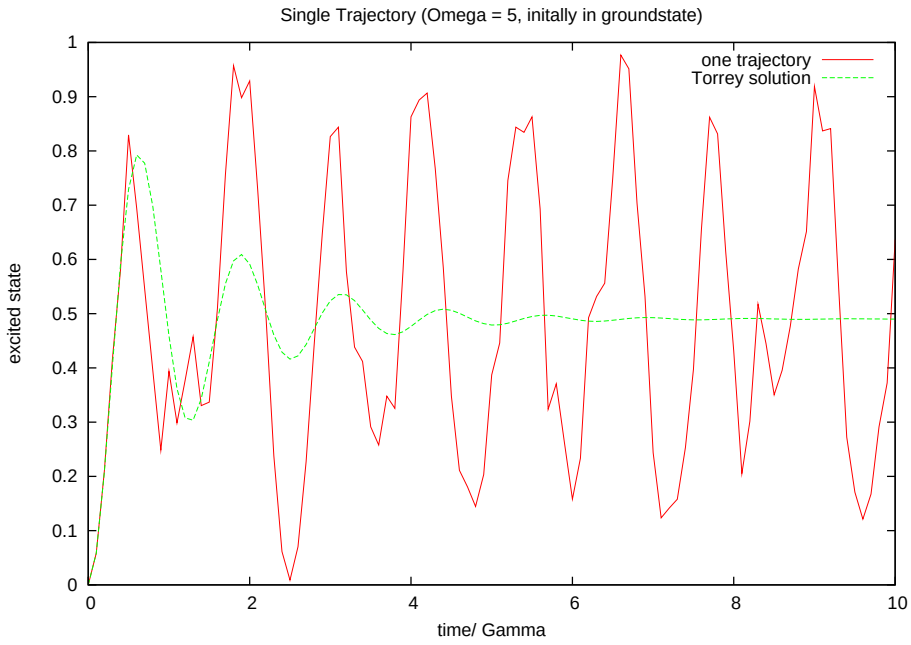

Figure 2: The excited state population for one trajectory for the SSE plotted contrast to the Torrey solution given $\Delta = 0$, $\Gamma = 1$ and $\Omega = 5$ with the atom initially in the ground state.

1.3 Analytic Comparison

Now we have a tool to numerically evolve the SSE and we will use it to create trajectories for a our SSE given above. It will be clear that the averaging over trajectories washes out the stochastic part of the of the SSE and in the large trajectory limit as is evident by the overall ensamble looking like the analytic solution. In our case we compared the ensamble of trajectories to the Torrey solution for the two-level atom. The Torrey solution is given by:

$$\begin{aligned}
\langle\sigma_x(t)\rangle &= 0 \\
\langle\sigma_y(t)\rangle &= \tfrac{\Omega\Gamma}{\Omega^2+\frac{\Gamma^2}{2}}\left[1 - e^{-\frac{3\Gamma}{4}t}\left(cos\Omega_\Gamma t - \tfrac{\Omega^2-\frac{\Gamma^2}{4}}{\Gamma\Omega_\Gamma} sin\Omega_\Gamma t\right)\right] \\
\langle\sigma_z(t)\rangle &= -1 + \tfrac{\Omega^2}{\Omega^2+\frac{\Gamma^2}{2}}\left[1 - e^{-\frac{3\Gamma}{4}t}\left(cos\Omega_\Gamma t + \tfrac{3\Gamma}{4\Omega_\Gamma} sin\Omega_\Gamma t\right)\right]
\end{aligned} \tag{8}$$

where

$$\Omega_\Gamma = \sqrt{\Omega^2 - \left(\frac{\Gamma}{4}\right)^2}. \tag{9}$$

To begin the comparison, one trajectory is shown in Figure **??** with the Torrey solution. Both have $\Delta = 0$, $\Gamma = 1$ and $\Omega = 5$ with the atom initially in the ground state. Clearly the noise imparted on a single trajectory deviates substatially from the analytic case. Upon averaging trajectories it is seen in Figure **??** that the washing out of noise is evident. As further comparison we evaluated the error, defined as the mean absolute difference of averaged trajectories to the Torrey solution. In Figure **??** the error verses trajectories averaged

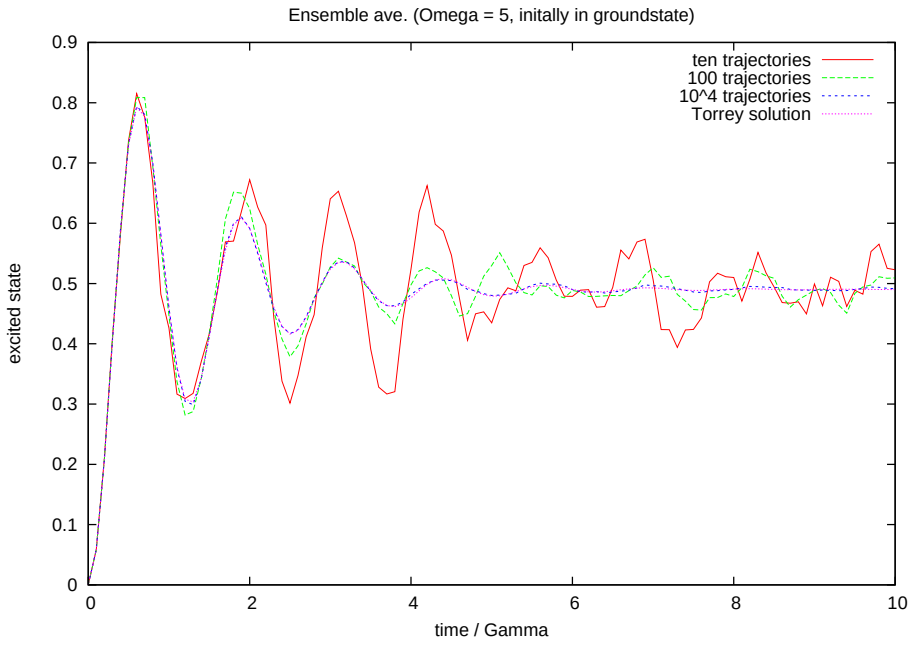

Figure 3: The excited state population for an ensemble of trajectories for the SSE plotted contrast to the Torrey solution given $\Delta = 0$, $\Gamma = 1$ and $\Omega = 5$ with the atom initially in the ground state.

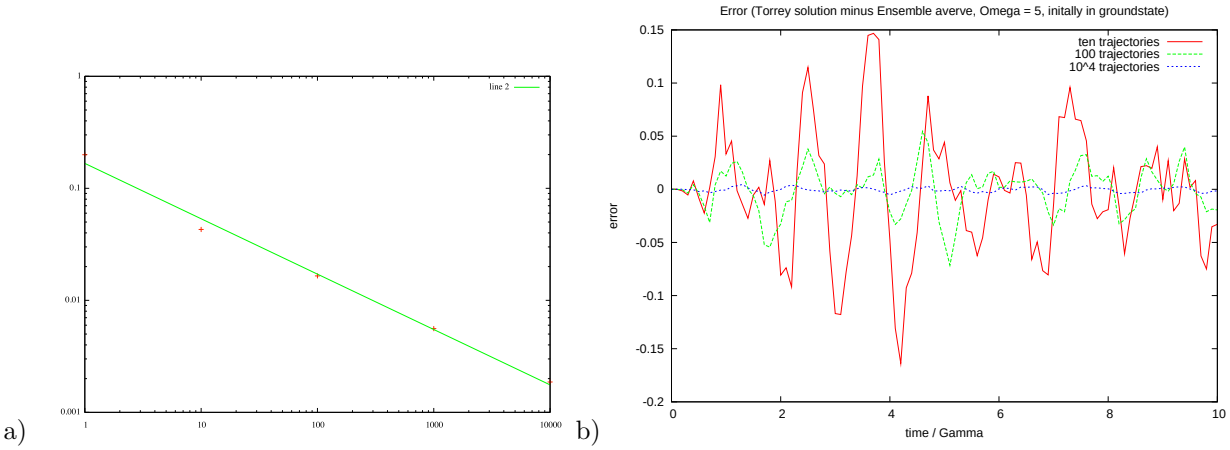

Figure 4: In figure a) the vertical axis is error, defined as the mean absolute difference of averaged trajectories to the Torrey solution, and the horizontal axis is the number of trajectories averaged n. The error verses trajectories averaged shows a decrease in error as the number of averaged trajectories increases, which goes as $\frac{1}{\sqrt{n}}$. Figure b) is the difference of the Torrey solution to the averaged trajectories plotted against time. Clearly the difference approaches zero as the number of trajectories averaged increases.

plot shows that the error decreases as the number of averaged trajectories increases. In fact it goes as $\frac{1}{\sqrt{n}}$. Where n is the number of trajectories averaged.

2 Numerical evolution of a quantum PDE

Consider a quantum one-dimensional simple harmonic oscillator. The Schrödinger equation for this system is given by:

$$i\hbar\partial_t\psi\left(x,t\right)=\left(\frac{p^2}{2}+\frac{1}{2}\omega^2x^2\right)\psi\left(x,t\right) \tag{10}$$

To time evolve the wave function $\psi\left(x,t\right)$ from t to t + Δt, one operates on the wave function by the operator $e^{-H\Delta t/\hbar}\psi\left(x,t\right)$:

$$\psi\left(x,t+\Delta t\right)=e^{iH\Delta t/\hbar}\psi\left(x,t\right) \tag{11}$$

Operating on a wave function in this manner is complicated. Instead, it is convenient to seperate the Hamiltonian into position and momentum operators:

$$H\left(x,p\right)=T(p)+V(x), \tag{12}$$

where T(p) is the kinetic energy term and V(x) is the potential energy term. The above exponential can then be expanded to different orders in Δt so that the position and momentum operators can operate on the wave function seperately. Two such expantions are as follows:

$$e^{-H\Delta t/\hbar}=e^{-iT(p)\Delta t/2\hbar}e^{-iV(x)\Delta t/\hbar}+O(\Delta t^2) \tag{13}$$

$$e^{-iH\Delta t/\hbar}=e^{-iV(x)\Delta t/2\hbar}e^{-iT(p)\Delta t/\hbar}e^{-iV(x)\Delta t/2\hbar}+O(\Delta t^3) \tag{14}$$

The derivations of these expansions follow. For simplicity, let $-iT(p)/\hbar\rightarrow A$ and $-iV(x)/\hbar\rightarrow B$. Then $H=A+B$, and we expand the following exponential to second order in Δt:

$$e^{(A+B)\Delta t}=1+A\Delta t+B\Delta t+O(\Delta t)^2 \tag{15}$$

One can see that this exponential has the same expansion to second order as:

$$e^{At}e^{Bt}=\left(1+A\Delta t+O(\Delta t)^2\right)\left(1+B\Delta t+O(\Delta t)^2\right)=1+A\Delta t+B\Delta t+O(\Delta t)^2 \tag{16}$$

Comparing these two expansions, we see, to second order, that:

$$e^{-H\Delta t/\hbar}=e^{-iT(p)\Delta t/2\hbar}e^{-iV(x)\Delta t/\hbar}+O(\Delta t^2) \tag{17}$$

Similarly, one can expand $e^{(A+B)\Delta t}$ to third order:

$$\begin{aligned} e^{(A+B)\Delta t} &= 1+(A+B)t+\tfrac{1}{2}(A+B)^2(\Delta t)^2+O(\Delta t)^3 \\ &= 1+A\Delta t+B\Delta t+\tfrac{1}{2}A^2(\Delta t)^2+\tfrac{1}{2}AB(\Delta t)^2+\tfrac{1}{2}BA(\Delta t)^2+\tfrac{1}{2}B^2(\Delta t)^2+O(\Delta t)^3 \end{aligned} \tag{18}$$

This exponential has the same expansion to third order as:

$$\begin{aligned} e^{B\Delta t/2}e^{A\Delta t}e^{B\Delta t/2}=&\left(1+\tfrac{1}{2}B\Delta t+\tfrac{1}{8}B^2(\Delta t)^2+O(\Delta t)^3\right)\left(1+A\Delta t+\tfrac{1}{2}A^2(\Delta t)^2+O(\Delta t)^3\right)\cdot \\ &\cdot\left(1+\tfrac{1}{2}Bt+\tfrac{1}{8}B^2(\Delta t)^2+O(\Delta t)^3\right) \\ =&\left(1+\tfrac{1}{2}\Delta t+\tfrac{1}{8}B^2(\Delta t)^2\right)\cdot \\ &\cdot\left(1+\tfrac{1}{2}B\Delta t+A\Delta t+\tfrac{1}{2}A^2(\Delta t)^2+\tfrac{1}{8}B^2(\Delta t)^2+\tfrac{1}{2}AB(\Delta t)^2\right)+O(\Delta t)^3 \\ =&1+B\Delta t+A\Delta t+\tfrac{1}{2}A^2(\Delta t)^2+\tfrac{1}{2}B^2(\Delta t)^2+\tfrac{1}{2}AB(\Delta t)^2+\tfrac{1}{2}BA(\Delta t)^2+O(\Delta t)^3 \end{aligned} \tag{19}$$

Comparing these expansions, we see that, to third order:

$$e^{-iH\Delta t/\hbar} = e^{-iV(x)\Delta t/2\hbar}e^{-iT(p)\Delta t/\hbar}e^{-iV(x)\Delta t/2\hbar} + O(\Delta t^3) \tag{20}$$

Although this last expansion has local error of order $(\Delta t)^3$, it has global error of order $(\Delta t)^2$ after many measurements. This is because each time one evolves the wave function from $\psi(x,t)$ to $\psi(x,t+\Delta t)$, one must act on it with $e^{-iV(x)\Delta t/2\hbar}e^{-iT(p)\Delta t/\hbar}e^{-iV(x)\Delta t/2\hbar}$. Everytime one does this, the $e^{-iV(x)\Delta t/2\hbar}$ from the previous evolution is sandwiched next to a $e^{-iV(x)\Delta t/2\hbar}$ from the current evolution. Thus, it appears that the exponential containing V(x) actually evolves the wave function by a whole time step before the T(p) exponential operates on it, which is the situation given by the previous expansion in which an error of order $(\Delta t)^2$ was returned.

The above expansions can be applied to time-dependent potentials with some appropriate changes. The time-evolution operator is then give by:

$$U(t,t+\Delta t) = exp\left[-\frac{i}{\hbar}\int_t^{t+\Delta t} dt' H(t')\right] \tag{21}$$

A simple expansion with decent accuracy is given by:

$$exp\left[-\frac{i}{\hbar}\int_t^{t+\Delta t} dt' H(t')\right] = e^{-iV(x,t)\Delta t/2\hbar}e^{-iT(p)\Delta t/\hbar}e^{-iV(x,t+\Delta t/2\hbar} + O(\Delta t)^3 \tag{22}$$

Once again, although the local error is of order $(\Delta t)^3$, the global error is of order $(\Delta t)^2$ after N measurements. According to Richardson's ansatz, the global error will then take the form:

$$\tilde{\psi}_{\Delta t}(x,t) - \psi(x,t) = e_2(x,t)(\Delta t)^2 + e_4(x,t)(\Delta t)^4 + e_6(x,t)(\Delta t)^6 + \ldots, \tag{23}$$

where $\psi(x,t)$ is the exact solution, $\tilde{\psi}_{\Delta t}(x,t)$ is the numerical approximation calculated using step sizes of Δt, and the $e_n(x,t)$ are coefficients independent of Δt. Only even order terms appear because it is important to preserve time-reversal symmetry. If going from t to t + Δt produces a given error, then going from t to t - Δt must remove the error terms. However, the odd order terms would have a sign different from the even order terms, effectively canceling some of the error and making the error in time reversal smaller than the original error. So, it is important to keep either all even or all odd terms. The even terms are the ones needed since the expansion utilized has a global error of order $(\Delta t)^2$ and therefore an error term of order 2 must appear.

Using Richardson extrapolation, higher order approximations can be achieved. The idea is to construct numerical solutions using different time steps, and then combine the solutions with appropriate weights to eliminate lower order terms. For example, fourth order approximation can be achieved as follows:

$$\begin{aligned}\tfrac{4}{3}\tilde{\psi}_{\Delta t/2}(x,t) - \tfrac{1}{3}\tilde{\psi}_{\Delta t}(x,t) &= \tfrac{4}{3}\psi(x,t) + \tfrac{4}{3}\left[e_2(x,t)\left(\tfrac{\Delta t}{2}\right)^2 + O(\Delta t)^4\right] - \tfrac{1}{3}\psi(x,t) - \tfrac{1}{3}\left[e_2(\Delta t)^2 + O(\Delta t)^4\right] \\ &= \psi(x,t) - \left(\tfrac{1}{3} - \tfrac{1}{3}\right)e_2(\Delta t)^2 + O(\Delta t)^4 \\ &= \psi(x,t) + O(\Delta t)^4\end{aligned} \tag{24}$$

A similar technique produces a sixth order expansion:

$$\begin{aligned}
\tfrac{1}{24}\tilde{\psi}_{\Delta t} - \tfrac{16}{15}\tilde{\psi}_{\Delta t/2} + \tfrac{81}{40}\tilde{\psi}_{\Delta t/3} = & \tfrac{1}{24}\left[\psi(x,t) + e_2(x,t)(\Delta t)^2 + e_4(x,t)(\Delta t)^4 + O(\Delta t)^6\right] \\
& -\tfrac{16}{15}\left[\psi(x,t) + e_2(x,t)\left(\tfrac{\Delta t}{2}\right)^2 + e_4(x,t)\left(\tfrac{\Delta t}{2}\right)^4 + O(\Delta t)^6\right] \\
& +\tfrac{81}{40}\left[\psi(x,t) + e_2(x,t)\left(\tfrac{\Delta t}{3}\right)^2 + e_4(x,t)\left(\tfrac{\Delta t}{3}\right)^4 + O(\Delta t)^6\right] \\
= & \left(\tfrac{1}{24} - \tfrac{16}{15} + \tfrac{81}{40}\right)\psi(x,t) + \left(\tfrac{1}{24} - \tfrac{4}{15} + \tfrac{9}{40}\right)e_2(x,t)(\Delta t)^2 \\
& + \left(\tfrac{1}{24} - \tfrac{1}{15} + \tfrac{1}{40}\right)e_4(x,t)(\Delta t)^4 + O(\Delta t)^6 \\
= & \psi(x,t) + O(\Delta t)^6
\end{aligned} \tag{25}$$

The time evolution of a quantum harmonic oscillator was calculated numerically using a stochastic integrator. The integrator has the ability to evolve the wave function using the 2nd order, 4th order, or 6th order approximations derived above.

For the second order, the expectation value of x, denoted $\langle x \rangle$, was compared to its exact solution. The exact solution is simply $\langle x \rangle = \cos(\omega t)$ since there is no damping, where ω is the natural frequency of the harmonic oscillator. The numerical solution was compared to this using 1000 data points by finding the magnitude of the difference between the numerical and exact solutions at each point and calculating its mean value. This was done for several different time steps. The log of the error is plotted versus the log of the time steps, and a linear fit was calculated to show the order at which the error increases for each time step. The plot looks like this:

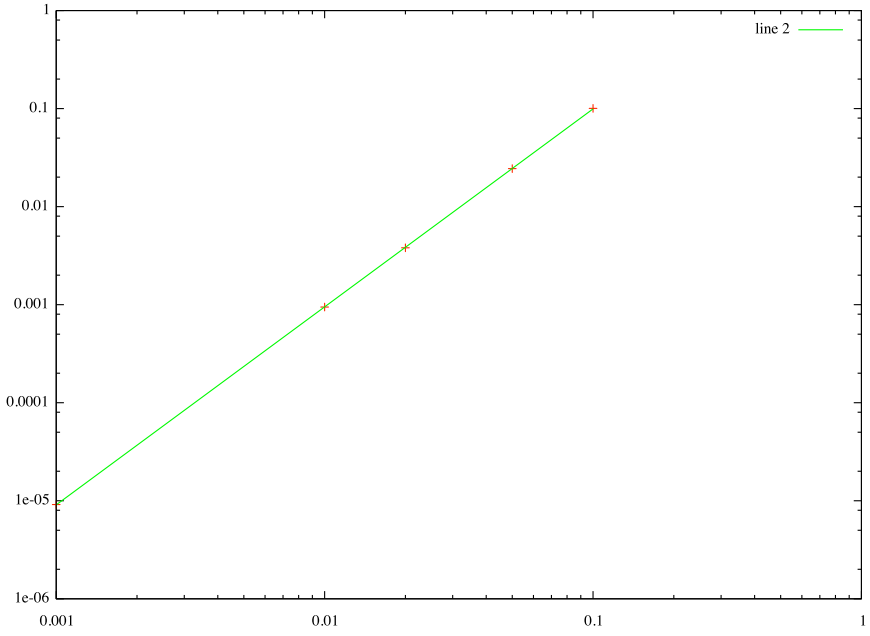

Figure 5: 2nd order log vs. log plot of error versus time step (slope of fit is 2.0)

Demonstrating the error with the higher order approximations is more difficult. The calculated $\langle x \rangle$ does not

demonstrate a significant enough amount of error to produce a plot like the second order one above. Instead, the norm of the wavefunction was calculated with the 4th and 6th order approximations. The norm should always be one, so the error was determined by finding the deviation of the norm from one for each time step. Even using this method, the error was too small to demonstrate a perfect 4th or 6th order fit. However, the increasing rank of the approximation is evident, as the 4th and 6th order error versus time step plots indicate.

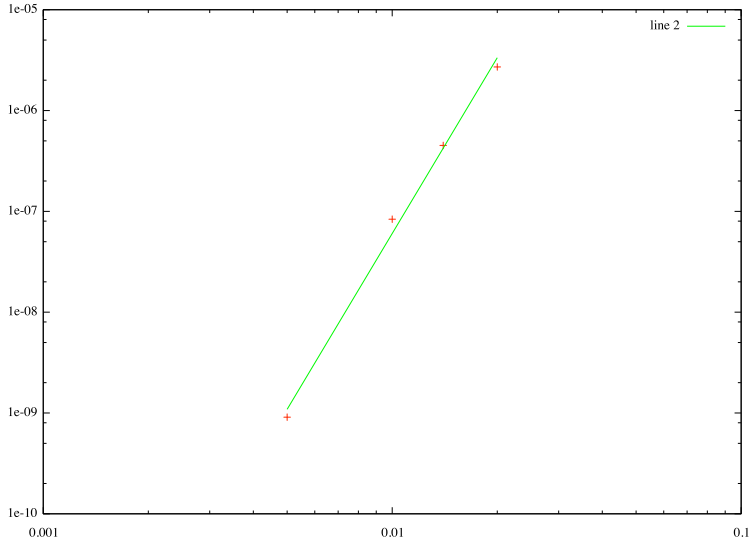

Figure 6: 4th order log vs. log plot of error versus time step (slope of fit is 5.8)

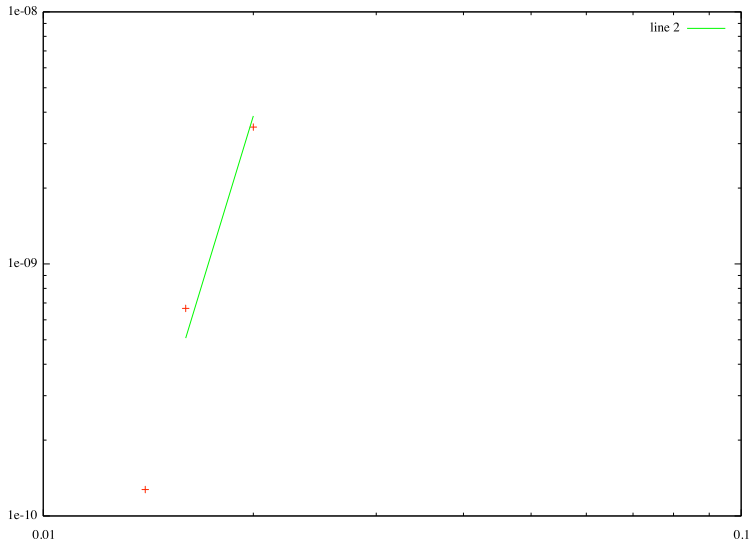

Figure 7: 6th order log vs. log plot of error versus time step (slope of fit is 9.1)

3 Quantum feedback control of the motion of a quantum-mechanical particle

3.1 Theory

It is possible to cool the temperature of an atom trapped in a quantum harmonic oscillator potential by manipulating the trap frequency at judicially chosen times. The frequency needs to be manipulated at specific times to obtain this cooling. It is necessary to know the position of the atom with some accuracy to choose the correct times to change the trap frequency. When the atom is near the center of the oscillator well, the trap frequency should be high, and when it is far from the well center, the trap frequency should be low. Changing the frequency in this way can remove energy from the particle. The optimum cooling process would implement a "bang-bang" approach, meaning the frequency of the oscillator is changed very suddenly when the atom reaches either of its desired positions. This approach is not necessary, however, and our approach uses a continuous, sinusoidal change of the trap frequency.

Consider a continuous measurement of the position of a one-dimensional harmonic oscilator. The master equation for this system is given by:

$$d\rho = -\frac{i}{\hbar}[H,\rho]dt + 2kD[x]\rho dt + sqrt2kH[x]\rho dW. \tag{26}$$

Take the Hamiltonian H to be the Hamiltonian of Problem 2, this form of the continuous-measurement master equation follows from taking the SME from Problem 1 and letting $\sigma \to x$ and $\Sigma \to 2k$. The SME can then be written in the equivalent form

$$d\rho = -\frac{i}{\hbar}[H,\rho]dt + k[x,[x,\rho]]dt + \sqrt{2k}([x,\rho]_+ - 2\langle x\rangle\rho)dW, \tag{27}$$

and then unravelled as the SSE

$$d|\psi\rangle = -\frac{i}{\hbar}H|\psi\rangle dt - k(x-\langle x\rangle)^2|\psi\rangle dt + \sqrt{2k}(x-\langle x\rangle)|\psi\rangle dW. \tag{28}$$

The corresponding measurement record follows from taking the homodyne photocurrent with the same operator and scalar replacements and then rescaling the result:

$$dy(t) = \langle x\rangle dt + \frac{dW}{sqrt8k}, \tag{29}$$

with k as the measurement strength. Thus the measurement record (the sequence of measurement results) contains information about the mean particle position, as well as quantum noise.

To model feedback control of the quantum system, we should use the position information from the measurement record dy to attempt to cool the particle, e.g., by modulating the trap frequency ω. The strategy we use here is called "box-time" filter, averaging dy over a certain amount of previous steps, where a judicious choice of the period of time that is averaged over is appreciated. What we did here is simply take advantage of integration loops between two neighboring outputs and taking that length of each loop as our "box-time".

As for measurement strength k, the wave packet will become very delocalized if a too low strength is chosen. Nor would a too large strength be a reasonable choice for the wave packet dynamics will become noisy due to the quantum measurement "backaction".

The time evolution of the wave function was modelled in the same way as in the above section titled "Numerical evolution of a quantum PDE", using the time-dependent potential approximation with global error of order $(\Delta t)^2$.

3.2 Results

The temperature of the system was monitored by calculating the energy of the system from the wave function of the system, since temperature and energy are directly proportional. In our units, the energy was given by:

$$E = \frac{1}{2}\left(\omega^2\langle x^2\rangle + \langle p^2\rangle\right). \tag{30}$$

The act of measuring the system introduces energy into the system which, without implementing the feedback loop, causes the system to heat up. When the feedback is implemented, the oscillator frequency changes in such a way that the atom energy decreases. The following graphs depict the harmonic oscillator system with identical parameters, with the exception that in one case the trap frequency is constant (i.e. feedback is not implemented) and in the other the feedback is implemented. Without feedback, the energy of the system increases because the measurement process introduces energy into the system. With feedback, the energy of the system decreases as predicted above. Figure 8 depicts the results for these two cases:

a)

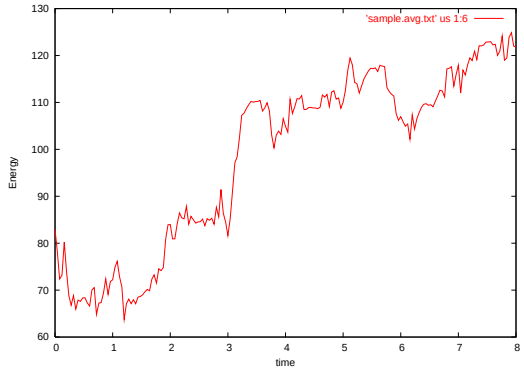

b)

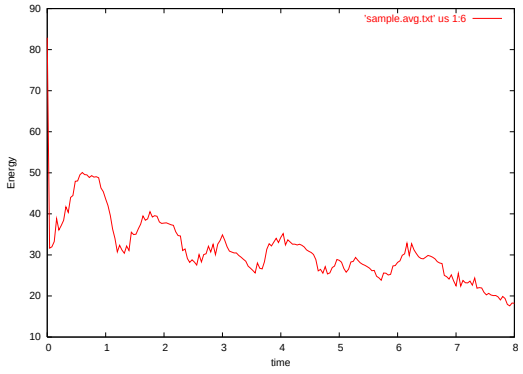

Figure 8: a) Energy of atom with no feedback b) Energy of atom with feedback

The energy appears to oscillate with the feedback because the potential is proportional to $\langle x\rangle^2$ which is changing from $\omega - \delta\omega$ to $\omega + \delta\omega$ continuously. However, the decreasing trend of the energy over time is appharent.

With feedback, as the energy of the system decreases, so does $\langle x\rangle$, $\langle y\rangle$, and the variances of x and y ($\sigma_x and \sigma_y$), as one would expect. Without feedback, these quantities increase over time. Figures 9 and 10 display the results.

Choosing the parameters to obtain cooling was difficult. We saw the most cooling when we chose the parameters $m = 1$ (mass), $k = 1$ (measurement strength), $\omega = 2\pi$ (oscillator frequency), $\langle x\rangle_o = 2.0$ (initial

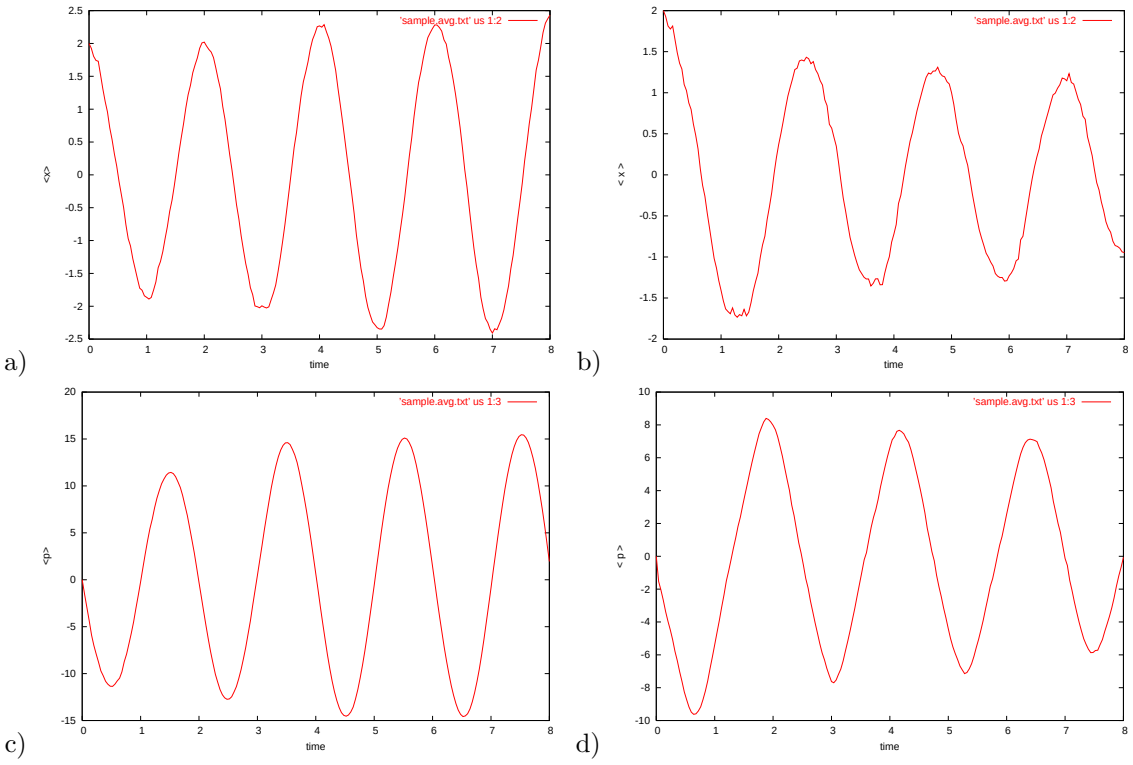

Figure 9: a) $\langle x \rangle$ without feedback b) $\langle x \rangle$ with feedback c) $\langle p \rangle$ without feedback d) $\langle p \rangle$ with feedback

expectation value of x), $\langle p \rangle_o = 0$, $\sigma_{x,o} = 0.4$, and $\sigma_{x,o} = 1.5$. Most of the other parameters chosen heated the system. Much more time and effort would be needed to find parameters that would optimize the cooling efficiency of this setup. However, the numerical solution provides evidence that cooling in this manner is possible.

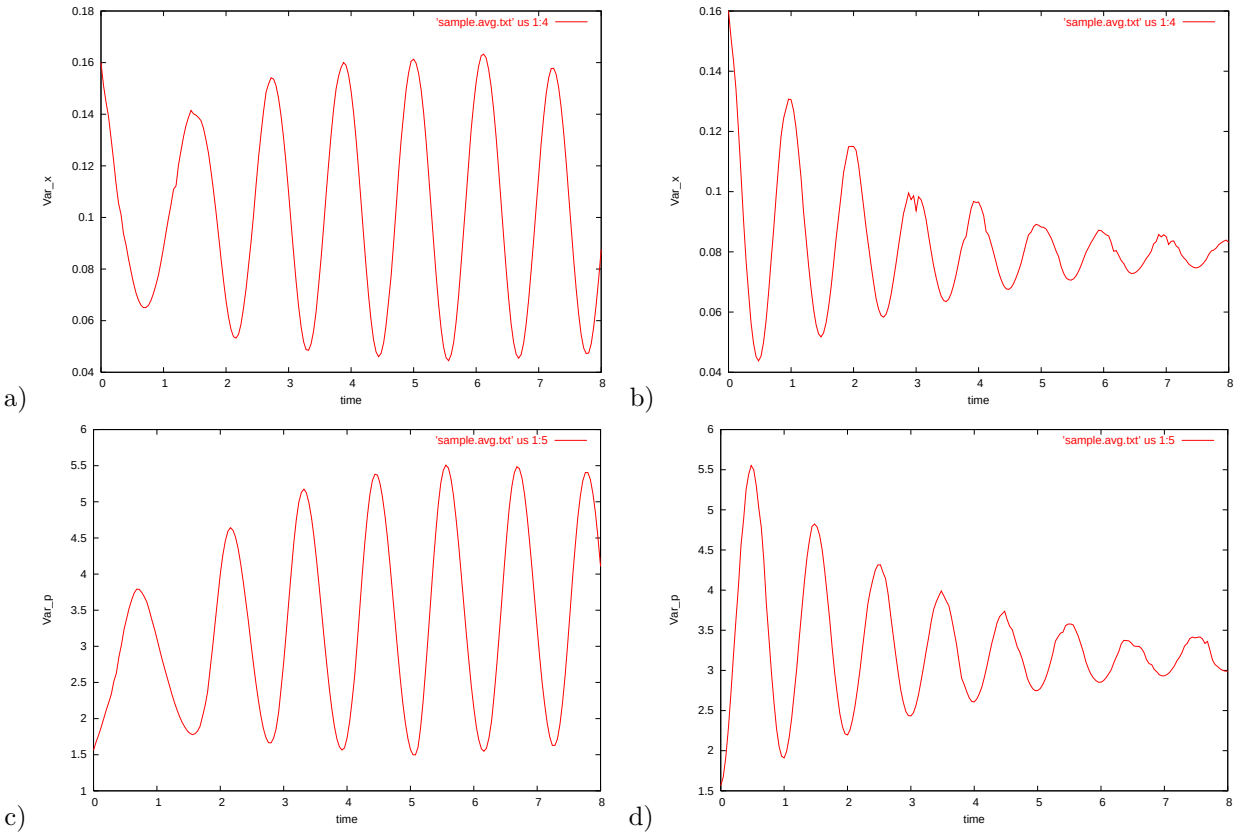

Figure 10: a) σ_x without feedback b) σ_x with feedback c) σ_p without feedback d) σ_p with feedback

4 Post Deadline Results

NOTE: system with measurement on with out feedback for 4 seconds, course cooling turned on for 12 seconds then fine cooling/trapping for remainder of time.

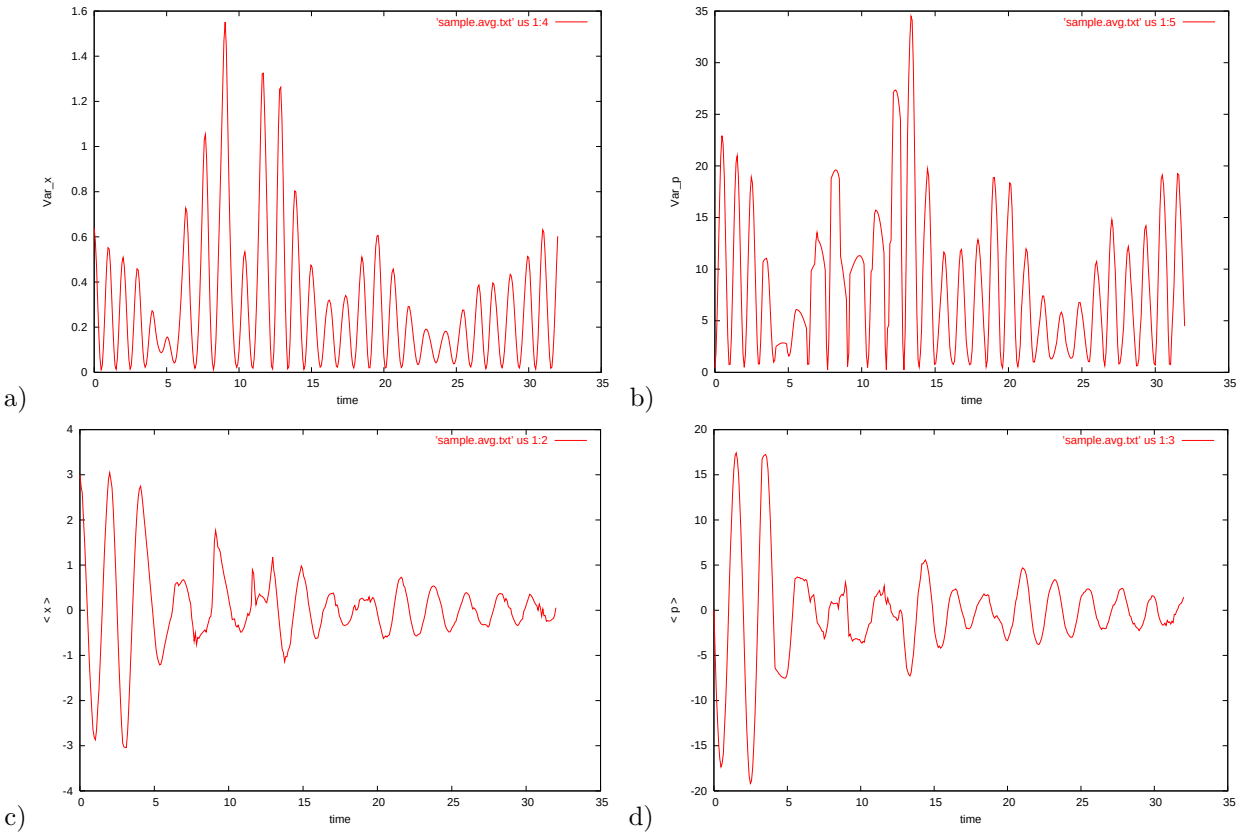

Figure 11: a) σ_x b) σ_p c) $\langle x \rangle$ d) $\langle x \rangle$.

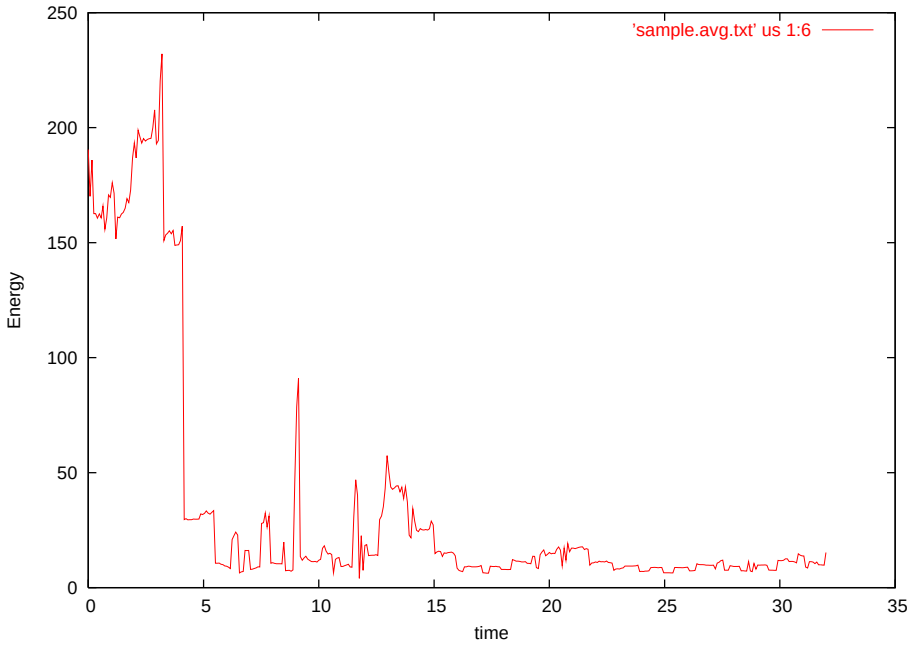

Figure 12: After several attempts at cooling using a feedback method where the potential was modulated continuously, proportional to the averaged value of the expectation value for x taken over fourty or so iterations, we decided to attempt a bang-bang approach. This time we had incredible results. The code averages previous expectation values for position to wash out the noise from measurement then changes the potetial when it computes the current position is closer to the origin than it is to the previous position and returns the potetial to the original value when it changes direction. This turns out to be a fairly powerful technique as can be seen in the energy.

References

[1] Claude Cohen-Tannoudji, "Atoms in strong resonant fields," in *Les Houches, Session XXVII, 1975 - Frontiers in Laser Spectroscopy*, R. Balian, S. Haroche, and S. Liberman, Eds. (North-Holland, Amsterdam, 1977).

[2] P. Marte, R. Dum, R. Taïeb, and P. Zoller, "Resonance fluorescence from quantized one-dimensional molasses," *Phys. Rev. A* **47**, 1378 (1993).